Two-Photon Absorption Long-Wavelength Optical Beam Tracking

Gerardo G. Ortiz* and William H. Farr*

A new optical beam tracking approach for free-space optical communication links using two-photon absorption (TPA) in a high-bandgap detector material was investigated. TPA is used to track a long-wavelength transmit laser while direct absorption on the same sensor simultaneously tracks a shorter-wavelength beacon. The TPA responsivity was measured for silicon using a PIN photodiode at a laser beacon wavelength of 1550 nm. As expected, the responsivity shows a linear dependence with incident power level. The responsivity slope is 5E-12 A/W/W/cm^2. Also, optical beam spots from the 1550-nm laser beacon were characterized on commercial charge-coupled device (CCD) and complementary metal-oxide semiconductor (CMOS) imagers with as little as 130 μW of optical power. This new tracker technology offers an innovative solution to reduce system complexity, improve transmit/receive isolation, improve optical efficiency, improve signal-to-noise ratio (SNR), and reduce cost for a free-space optical communications transceiver.

I. Introduction

Free-space optical communications requires accurate laser-beam pointing to achieve high data rates at low power levels [1,2]. For the most precise pointing, a beacon emanating from the receiver location must be acquired and tracked by the remote transceiver to obtain accurate knowledge of the receiver position. Simultaneously, the transceiver's outgoing transmit beam direction needs to be measured to accurately point to the receiver, including any required point-ahead angle to compensate for predicted movement of the receiver during the return transit time. The average power of the received beacon may be on the order of picowatts, whereas the average power of the transmit laser is on the order of watts.

The remote transceiver beacon acquisition and tracking detector should have high efficiency and low noise, and be low cost (e.g., silicon-based detectors). A single detector to track both the beacon and transmit laser is preferred, to reduce complexity and minimize alignment errors. State-of-the-art, high-power, efficient beacon lasers are presently available near 1064 nm [3]. However, transmit lasers currently baselined for deep-space links operate at a longer wavelength band, around 1550 nm [4,5]. At that wavelength, silicon is "blind" (with a bandgap ∼1150 nm) and cannot conventionally be used as the tracking sensor.

*Communications Architectures and Research Section.

The research described in this publication was carried out by the Jet Propulsion Laboratory, California Institute of Technology, under a contract with the National Aeronautics and Space Administration.

The use of two-photon absorption (TPA) for optical beam tracking is investigated here to change this conventional disadvantage into a practical solution that reduces system complexity, improves transmit/receive isolation, improves optical throughput, improves signal-to-noise ratio (SNR), and reduces cost.

Previous investigations of TPA have recognized that detector arrays can be applied to imaging and detection of ultrashort pulses in the infrared region [6]. Current research is seeking to exploit TPA for autocorrelation of ultrafast infrared laser pulses in silicon [7,8], single-shot sonogram generation for fast pulse diagnostics [9], absorption and Kerr coefficient measurement for bulk silicon in the 850 to 2200 nm band [10], and ultrafast all-optical modulation in silicon-on-insulator waveguides [11].

II. TPA Optical Beam Tracker

The use of TPA in a high-bandgap detector material (e.g., silicon) to track a long-wavelength transmitter laser (e.g., 1550 nm) while simultaneously using direct absorption on the same sensor to track a shorter-wavelength beacon (e.g., 1000 nm) is depicted in Figure 1. The use of two-photon and direct absorption in a single sensor requires only one optical channel for tracking, thereby improving optical efficiency and reducing size, mass, and power. Also, keeping the wavelengths widely separated dramatically improves the transmit/receive isolation, especially since efficient TPA requires a tightly focused beam, such that scattered light will not affect the tracking SNR.

The TPA tracking concept is not limited to these specific wavelengths nor to silicon as the sensor material. The tracking concept can be applied to other transmitter and beacon wavelengths where the transition between the long and the short wavelength is set by the bandgap of the sensor. For example, in silicon the bandgap is 1.11 eV, and therefore the transition wavelength is 1150 nm. A detector fabricated from indium gallium arsenide phosphide (InGaAsP) with a bandgap of 0.95 eV would result in a transition wavelength at 1300 nm. This material would result in higher quantum efficiency than silicon at a beacon wavelength of 1064 nm, but with lower device noise than InGaAs due to its larger bandgap.

A previous approach for deep-space tracking proposed using an indium gallium arsenide (InGaAs) focal-plane array sensor with direct absorption at both the transmitter and beacon wavelengths [12], but this solution incurs a noise penalty from higher dark current due to the lower bandgap, reducing the system SNR. Another possible approach would utilize two separate sensors — silicon for beacon tracking and InGaAs for transmitter tracking. This optimizes the SNR for both beams at the cost of a second sensor, a second optical channel, more electronics, and alignment complexity.

To validate the TPA tracking concept, we show in this article that less than 0.1 mW of 1550-nm transmit laser power is sufficient to generate a transmit spot with enough signal to track the beam on a commercially available, low-cost silicon charge-coupled device (CCD) camera. This power level is 0.01 percent of a typical 1-W communications transmit laser optical power.

As an example of the TPA beam tracker, consider a silicon-based, pixellated N×N focal plane array (e.g., CCD, active pixel sensor, or complementary metal-oxide semi-conductor) upon which both the short-wavelength beacon (e.g., 1064 nm) and a small part (~ 0.1 mW) of the long-wavelength transmit laser (e.g., 1550 nm) are focused. The focused spots are offset from each other to avoid overlapping. If necessary, modulation on the beams can be used to remove ambiguity between the spots. Because silicon's direct absorption bandgap (Eg = 1.11 eV) is lower than the energy of the beacon photons (e.g., photons at 1000 nm have an energy of 1.24 eV), the sensor can absorb the photons directly and generate free carriers in the incident pixels that are representative of the photon flux. The generated charge in these pixels is collected, transferred, and measured by the readout electronics, thereby yielding an image of the beacon spot.

Simultaneously, on a different region of the array, the long-wavelength photons, with their lower energy level (e.g., photons at 1550 nm have an energy of 0.8 eV), cannot be directly absorbed by the sensor. However, in the nonlinear TPA process, a single electron-hole pair can be produced by the virtual simultaneous absorption of two photons. The photocurrent generated is proportional to the square of the incident optical intensity [13]. Once the charge is generated, it is collected, transferred, and measured by the detector readout electronics.

The optical beam tracker reads out the pixels from the array, yielding an image with the two spots. It computes the spots' centroids and determines the beacon and the transmit locations. This information is used to track the two spots and to precisely point the transmit communication laser beam to the receiver.

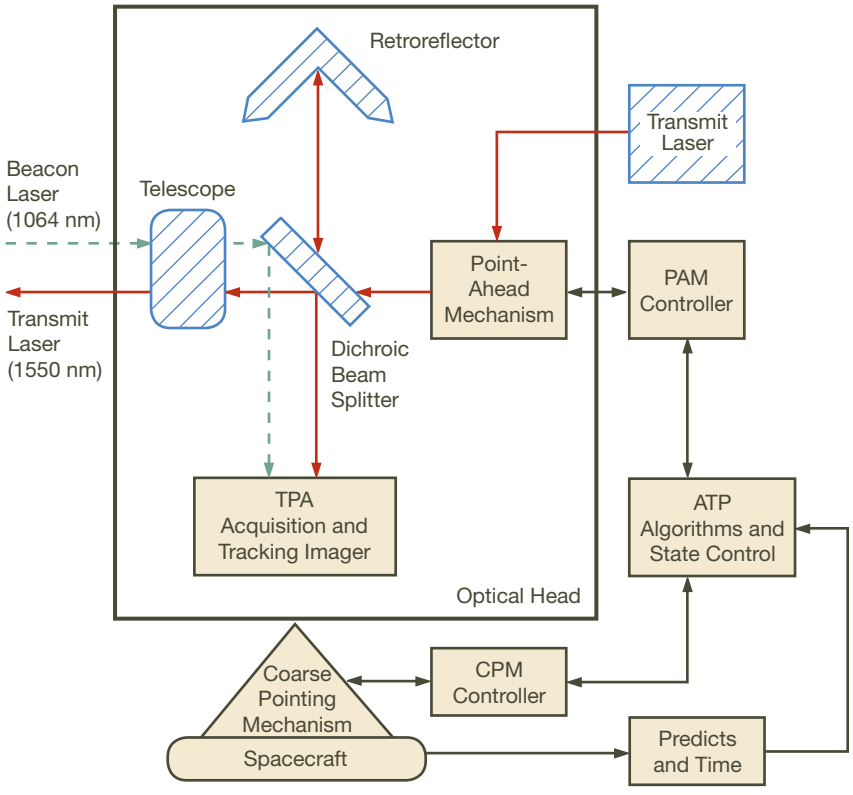

Figure 1. TPA long-wavelength optical beam acquisition, tracking, and pointing (ATP) system.

Note that this tracking scheme also allows for efficient tracking of the Earth irradiance as a beacon source due to the higher quantum efficiency (QE) of the silicon sensor in the visible regime for reflected sunlight. It also enables tracking using a combination of a laser beacon and an Earth irradiance beacon.

III. TPA Responsivity

Consider a beam of photons incident on a semiconductor detector. When the energy of the photon, $h\nu$, is less than the detector bandgap, E_g, one photon cannot provide sufficient energy to raise an electron from the valence band to the conduction band to generate a free-charge carrier. This detector is "blind" to photons of lower energy than that gap. Nevertheless, if the bandgap is less than $2h\nu$, two of these photons can occasionally create a virtual intermediate state to jointly transfer their energy to create an electron-hole pair. The absorption coefficient for this process is proportional to the intensity of the light, which means that the photocurrent generated is proportional to the square of the incident optical density [13].

The responsivity, $\Re$, of a detector relates the electric current, i, flowing in the device to the incident optical power, P, such that $\Re = i/P$.

The current density induced by the TPA process is given by

$$J_P = \zeta\phi^2$$

from [14], where ζ is a material constant and ϕ is the photon flux density (photons/cm^2/sec) with energy $h\nu$.

The responsivity of the TPA process is then

$$\Re = \frac{i}{P} = \frac{i/A}{P/A} = \frac{J_P}{P/A} = \frac{\zeta\phi^2}{P/A}$$

Since the optical power is $P = h\nu(\phi A)$, where A is the area, then

$$\Re = \left[\frac{\zeta}{(hc)^2}\right]\lambda^2\frac{P}{A} \tag{1}$$

This relationship shows that the TPA responsivity increases linearly with incident power level, and is inversely proportional to the area of absorption. This favors a high response from tightly focused spots. It is desirable to minimize the amount of signal taken from the transmitter in order to perform the tracking function. Thus, the responsivity as a function of incident power level for several detector types was assessed to demonstrate the ability to generate sufficient photoelectron carriers to observe a spot on a pixellated focal plane array.

IV. Photoelectron Generation Rate Measurement

The dependence of the photoelectron generation rate on the incident power level due to TPA was investigated by tightly focusing a 1550-nm, high-power laser beam on a silicon PIN photodiode.

A photograph of the test set-up is shown in Figure 2. The master oscillator laser is a 10-mW, 1550-nm Fabry-Perot diode laser used as a seed into a 2-W fiber amplifier. The high-power signal is routed via a single-mode fiber into a collimator to generate a 10-mm-diameter beam. The beam passes through a bandpass filter with a central peak at 1546.0 nm (bandwidth of 79.4 nm) to remove any residual pump power leaking from the fiber amplifier. The beam then traverses through two neutral-density (ND) filters on rotating wheels to vary the incident signal level on the detector. The ND filters are Inconel® metallic coatings on a glass substrate with a flat transmission response from 400 to 2500 nm. The range of optical densities varies from 0.08 to 3.0. A removable beam block is used to block the laser signal between measurements to reduce Joule heating effects. The 10-mm beam is focused on the detector with a 20× apochromatic near-infrared objective with a numerical aperture of 0.4 and a 20-mm working distance. The transmission efficiency of this objective is ~55 percent at 1550 nm.[1] To remove ambient light noise, the room lights are turned off during experiments. A long-pass filter with a cutoff wavelength at 1050 nm is placed in front of the detector and the detector is mounted on an XYZ stage for positioning and focusing. The detector current is sensed by a picoammeter with 1-pA RMS noise.

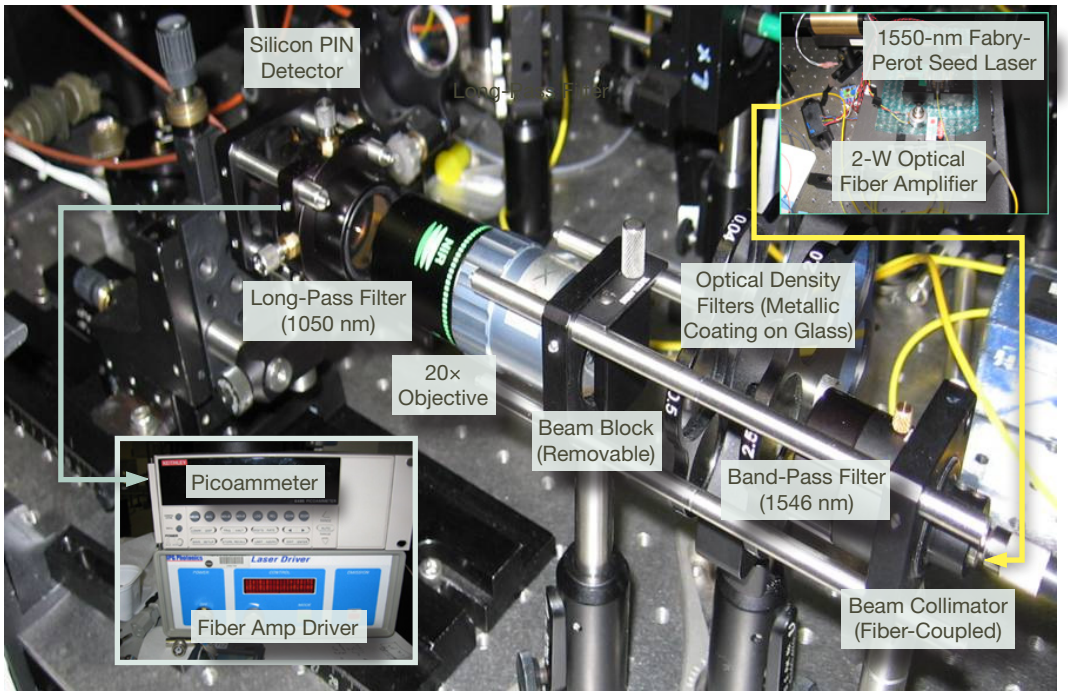

Figure 2. Setup for testing TPA in silicon PIN diode. The 1550-nm amplified laser power from a Fabry-Perot seed laser is focused on the detector with a 20× objective.

[1] Mitutoyo M Plan Apochromatic 20× Objective.

The detector has a 1.02 mm diameter with a spectral sensitivity response from 200 to 1100 nm — see Figure 3.[2] During these tests, the detector was operated in the unbiased photovoltaic mode to keep dark current to a minimum. The dark current in this mode was measured to be below 10 pA in non-illuminated conditions at room temperature. The

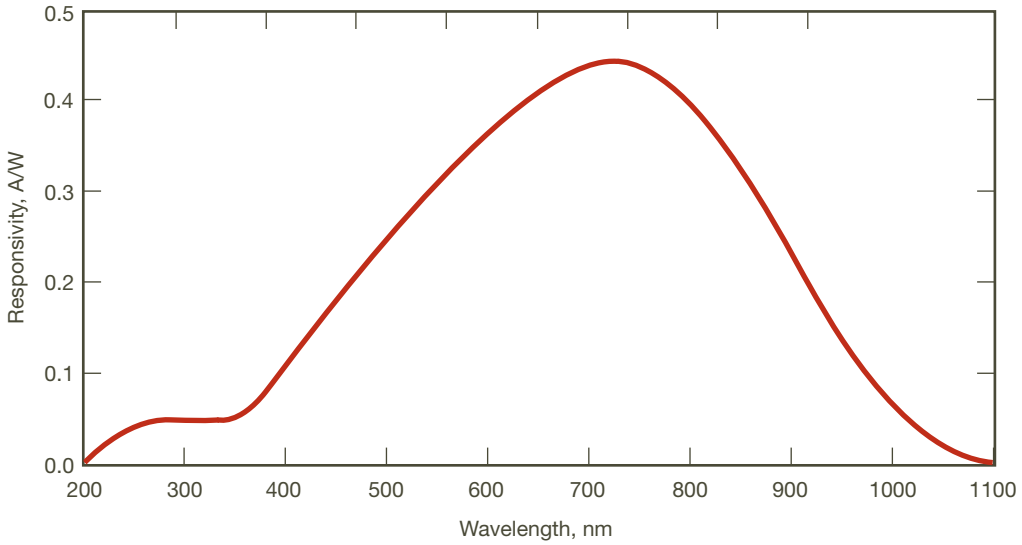

Figure 3. Spectral responsivity curve of the silicon PIN detector used in the experiment. The detector is sensitive to light from 200 to 1100 nm. The detector was operated in photovoltaic mode with a dark current of less than 10 pA.

linearity of the photovoltaic mode was verified with incident laser light at a wavelength of 633 nm.

To verify that the signal observed in the silicon detector was only due to the 1550-nm laser light, the optical spectrum was measured at the detector focal plane (Figure 4) by coupling to a fiber into the spectrum analyzer. The optical spectrum was measured from 600 to

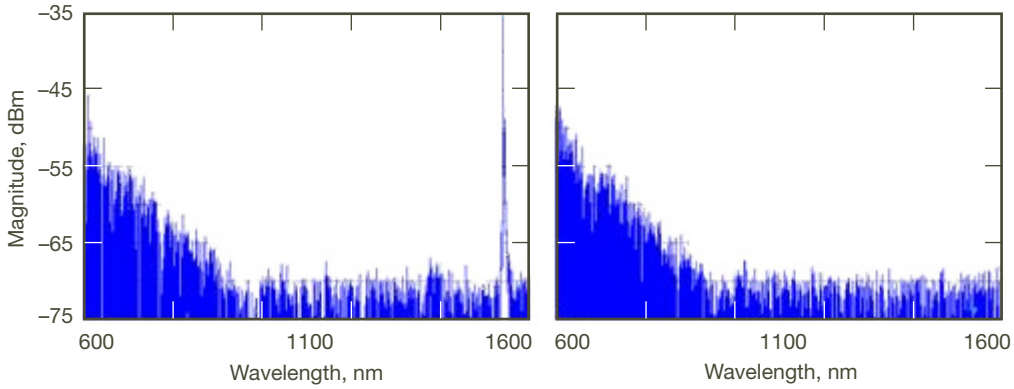

(a) Spectral measurement of signal incident at the detector focal plane.

(b) Calibration of optical spectrum analyzer: measurement with no input signal.

Figure 4. Spectral measurement of the incident signal at the focal plane. The incident laser power is filtered at 1541.6 nm with no signal observed elsewhere in the spectral band.

[2] Thorlabs silicon PIN photodiode detector m/n FDS010.

1600 nm. The only observed signal was the laser signal at 1541.6 nm. The high noise levels from 600 to 900 nm were verified as due to the noise floor of the optical spectrum analyzer itself.

The test procedure involved calibrating the power level at the focal plane, optimizing the focus of the beam on the detector, and measuring the detector current as a function of incident power level.

The power level at the detector focal plane was calibrated with a thermal power meter as a function of the ND filter wheel positions. The power meter has a maximum power rating of 50 W and an uncertainty of measurement of ± 2.5 percent. The measured power ranged from 2 to 780 mW.

Placing the detector surface at the focal plane of the objective is a critical step to obtaining two-photon current generation. Slightly offsetting the detector surface from the focal plane would not produce a current response from the detector. The placement of the detector surface on the focal plane was determined by optimizing the current generated by the incident beam. Care was taken to optimize this placement at a low incident power level (~ 80 mW) to avoid generating current due to heating effects. The spot size at focus was estimated to be ~ 40 μm in diameter by the knife-edge method.

Heating effects were noticed when the detector was continually exposed to the laser beam. The current value increased with exposure duration. This was very dependent on power levels, being clearly obvious at the highest power and negligible at the low power levels. Therefore, a beam block was introduced to control the exposure time. The incident signal level was varied by rotating the ND filter wheels and the observed current was recorded.

The measured responsivity of the silicon PIN is plotted in Figure 5. For a direct absorption process, the responsivity is constant as a function of power. But here, the responsivity is

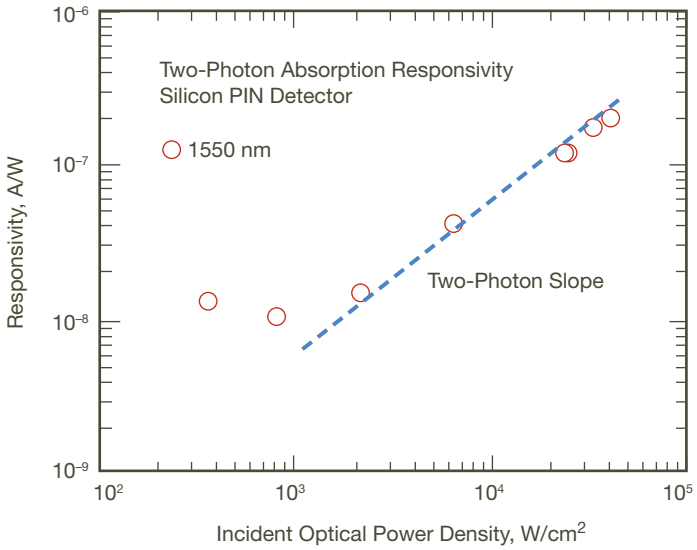

Figure 5. Responsivity of silicon PIN detector at 1550 nm. Responsivity shows linear dependence on incident power density, indicative of TPA.

observed to have a linear dependence with incident power level in agreement with Equation (1), thereby confirming the generation of photoelectron carriers by the TPA process. The slope of the responsivity was measured at 5E-12 A/W/W/cm^2.

The corresponding photoelectron generation rate as a function of power is plotted in Figure 6. Very high electron rates can be obtained — but how low can an incident power level be in order to track a spot on a silicon imager array?

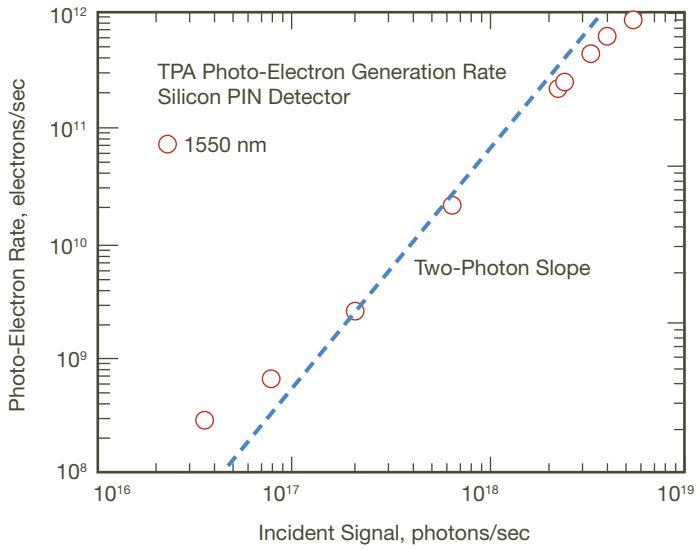

Figure 6. Photoelectron generation rate due to 1550-nm optical signal on silicon detector.

Using a typical CCD or CMOS imager, with a full well of 1E6 electrons per pixel, and a spot size that covers a 3×3 pixel area, approximately 5E6 electrons would be needed to track the spot. (This assumes that the pixels are only filled to 50 percent of capacity.) With a reasonable integration time of 100 ms, the photoelectron flux needed would be 5E7 electrons per sec, which can be obtained with a submilliwatt incident power level, as seen in Figure 6.

V. TPA-Imaged Spot on Silicon Camera

The amount of 1550-nm transmit laser power required to generate a spot on an N×N pixellated imager was investigated for two commercial silicon imagers: a silicon CCD camera and a silicon CMOS camera.

The setup comprised similar optics and focusing as in Figure 2, with the PIN detector replaced by the camera sensors. Also, since the previous measurement showed that low power levels would be sufficient to generate sufficient photoelectrons in the pixels to image the spot, the laser was replaced with a lower power (40 mW) fiber-coupled, single-mode, distributed-feedback (DFB) 1550-nm laser. This also allowed the ND filter wheels to be replaced by an in-line variable fiber attenuator and a 90/10 fiber splitter to monitor the power level.

The test procedure steps were to calibrate the optics insertion losses, optimize the camera sensor position to the focal plane, and then sample the image at various power levels.

The optics insertion losses were calibrated from the laser insertion point to the sensor focal plane. The throughput at 1550 nm was measured at 55 percent. Again, the TPA process was very sensitive to positioning of the camera's sensor surface at the focal plane of the objective. To optimize the placement of the sensor, the imager was run continuously, while the maximum signal level was observed as a function of position. This was done with a few milliwatts of total power.

A. A 1550-nm Laser Beam Imaged on a CCD Camera

The CCD image of the 1550–nm spot at two power levels is presented in Figure 7. The frame update rate was 30 Hz. The commercial silicon CCD camera used has a format of 1392 × 1040 pixels with a pixel pitch of 6.45 by 6.45 μm and an integrated 10-bit A/D converter. The 1550-nm laser imaged spot is clearly observed at these low power levels.

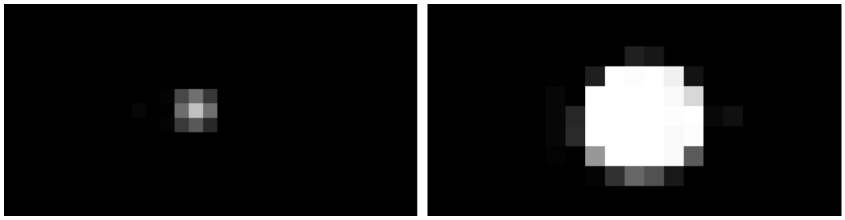

(a) 3.3 mW at 30 Hz (b) 12.5 mW at 30 Hz

Figure 7. Silicon CCD image of 1550-nm laser spot at incident power levels of 3.3 mW and 12.5 mW.

A profile of the spot at various power levels is shown in Figure 8. A 20 × 20 window is used for each profile. With the incident power at 6.6 mW and 12.5 mW, the pixels become saturated at 1024 DN (digital number). At a signal level of 3.3 mW, the central pixel is below saturation with a level of ~ 750 DN. Further reducing the power to 2.6 mW still shows a number of pixels collecting charge in the image of the spot with the central pixel ~ 350 DN.

B. A 1550-nm Laser Beam Imaged on a CMOS Camera

In Figure 9, the image of the 1550-nm spot on the CMOS silicon camera is displayed for two incident power levels. This commercial camera has a format of 1600 × 1200 pixels with a pitch of 2.8 μm × 2.8 μm. The sample rate for these images was 15 Hz. The camera has an integrated 8-bit A/D converter. The spot generated by TPA is shown for an incident power level of 548 μW, and is still clearly visible for an even lower power level of 128 μW.

Figure 10 shows the profile of the spot at various incident power levels. Zooming the spot to a 40 × 40 window displays the saturated pixels (DN = 256) with signal power levels greater than 128 μW. The spot becomes minimally detectable at a signal level of 13.7 μW — see Figure 10(d). The greater sensitivity of the CMOS camera to the TPA was likely due to better focusing.

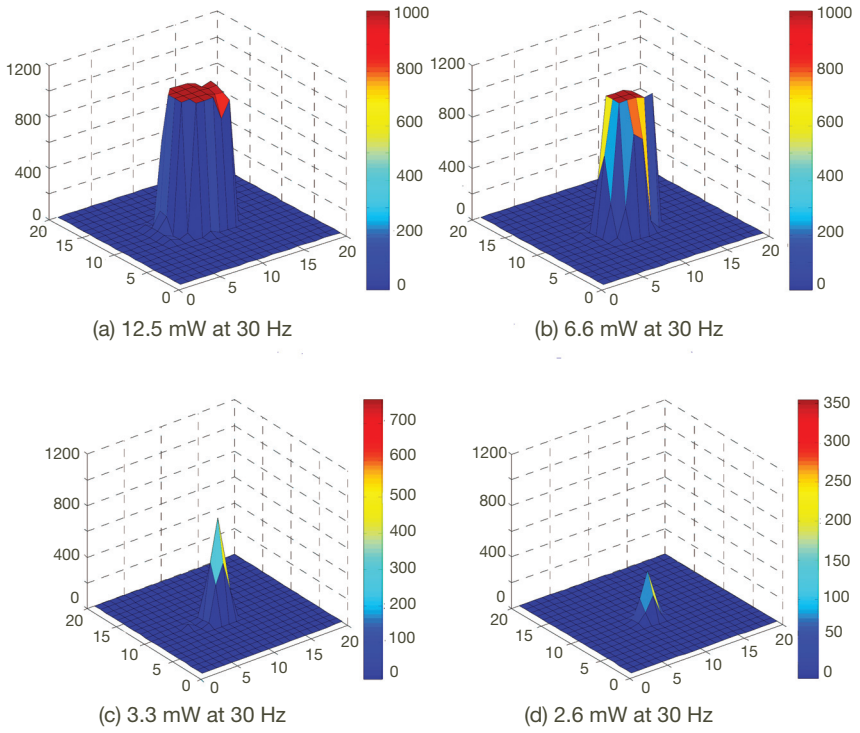

Figure 8. Spot profiles of 1550-nm laser spot on silicon CCD with varying incident power level at a constant integration time; 30 Hz is the full frame update rate.

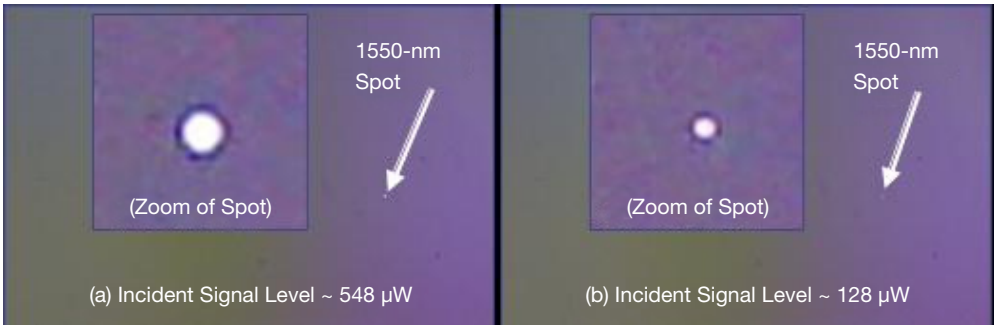

Figure 9. Silicon CMOS image of 1550-nm laser spot at two incident power levels.

VI. Conclusion

Dual-wavelength optical beam tracking by the use of TPA for free-space optical communication links has been proposed and investigated. The novelty in this technology is the simultaneous use of TPA for the long-wavelength transmitter laser signal and direct absorption for the short-wavelength beacon laser signal in a single sensor to track the optical beams. This is the first time TPA has been used for optical beam tracking, and this is the first time that TPA and direct absorption have been combined in a single sensor for imaging and optical beam tracking.

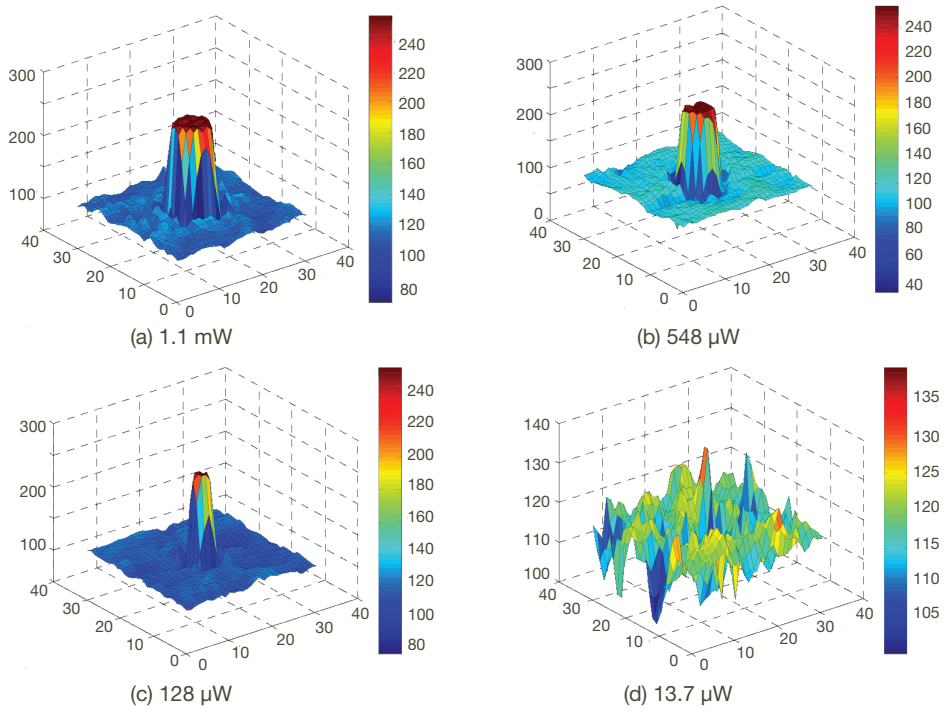

Figure 10. Profiles of 1550-nm spot on silicon CMOS detector at various power levels. Note that the spot is clearly observed with 128 µW total incident power. The frame rate is 15 Hz.

The TPA responsivity was measured for silicon using a PIN photodiode. As expected, the responsivity shows a linear dependence with incident power level. The responsivity was characterized with a slope of 5E-12 A/W/Wcm^2. Furthermore, the TPA response could be obtained with power levels of less than 1 mW, justifying the use as an optical beam tracker. Also, optical beam spots from a 1550-nm laser source were characterized on a CCD and a CMOS imager. As little as 130 µW of optical power was sufficient to saturate camera pixels and provide a distinct spot image.

This technology is directly applicable to free-space optical communication systems. For instance, this technology provides for a reduced complexity and reduced-cost optical beam tracking system, compared to the previously proposed Mars Laser Communication Demonstration Project. Currently, this technology is being integrated into a next-generation deep-space optical communication Mars prototype flight terminal by JPL's Optical Communications Group. It is also being considered for Earth orbiters, lunar optical transceivers, and planetary orbiters.

Acknowledgments

The authors gratefully acknowledge the use of the high-power lasers, optical laboratory, and equipment made available by Dr. Malcolm Wright, the helpful discussions with Jeffrey Charles, and the support provided by the members of the Optical Communications Group.

References

[1] H. Hemmati, ed., *Deep Space Optical Communications*, New York: John Wiley and Sons, Inc., 2006.

[2] S. Lee, J. W. Alexander, and G. G. Ortiz, "Sub-microradian Pointing System Design for Deep-Space Optical Communications," in Free-Space Laser Communication Technologies XIII, G. Stephen Mecherle, ed., *Proceedings of SPIE*, vol. 4272, pp. 104–111, January 2001.

[3] K. E. Wilson, M. Wright, R. Cesarone, J. Ceniceros, and K. Shea, "Cost and Performance Comparison of an Earth-Orbiting Optical Communication Relay Transceiver and a Ground-Based Optical Receiver Subnet," *The Interplanetary Network Progress Report*, vol. 42-153, Jet Propulsion Laboratory, Pasadena, California, pp. 1–12, May 15, 2003. http://ipnpr.jpl.nasa.gov/progress_report/42-153/153B.pdf

[4] G. G. Ortiz, M. Jeganathan, J. V. Sandusky, and H. Hemmati, "Design of a 2.5 Gbps Optical Transmitter for the International Space Station," in Free-Space Laser Communication Technologies XI, G. Stephen Mecherle, ed., *Proceedings of SPIE*, vol. 3615, pp. 179–184, 1999.

[5] S. A. Townes, B. L. Edwards, A. Biswas, D. R. Bold, R. S. Bondurant, D. Boroson, J. W. Burnside, D. O. Caplan, A. E. DeCew, R. DePaula, R. J. Fitzgerald, F. I. Khatri, A. K. McIntosh, D. V. Murphy, B. A. Parvin, A. D. Pillsbury, W. T. Roberts, J. J. Scozzafava, J. Sharma, and M. Wright, "The Mars Laser Communication Demonstration," in *IEEE Aerospace Conference Proceedings*, vol. 2, pp. 1180–1195, March 6–13, 2004.

[6] Y. Takagi, T. Kobayashi, and K. Yoshihara, "Multiple- and Single-Shot Autocorrelator Based on Two-Photon Conductivity in Semiconductors," *Optics Letters*, vol. 17, no. 9, pp. 658–660, May 1, 1992.

[7] K. A. Briggman, L. J. Richter, and J. C. Stephenson, "Imaging and Autocorrelation of Ultrafast Infrared Laser Pulses in the 3–11 μm Range with Silicon CCD Cameras and Photodiodes," *Optics Letters*, vol. 26, no. 4, pp. 238–240, February 15, 2001.

[8] P. G. Chua, Y. Tanaka, M. Takeda, and T. Kurokawa, "Infrared Image Detection with Si-CCD Image Sensor due to Two-Photon Absorption Process," in 4th Pacific Rim Conference on Lasers and Electro-Optics, pp. I-482–3, vol. 1, 2001.

[9] D. Panasenko and Y. Fainman, "Single-Shot Sonogram Generation for Femtosecond Laser Pulse Diagnostics by Use of Two-Photon Absorption in a Silicon CCD Camera," *Optics Letters*, vol. 27, no. 16, pp. 1475–1477, August 15, 2002.

[10] A. D. Bristow, N. Rotenberg, and H. M. van Driel, "Two-Photon Absorption and Kerr Coefficients of Silicon for 850–2200 nm," *Applied Physics Letters*, vol. 90, no. 19, 2007.

[11] D. J. Moss, L. Fu, I. Littler, and B. J. Eggleton, "Ultrafast All-Optical Modulation via Two-Photon Absorption in Silicon-on-Insulator Waveguides," *Electronics Letters*, vol. 41, no. 6, March 17, 2005.

[12] J. W. Burnside, D. V. Murphy, F. K. Knight, and F. I. Khatri, "A Hybrid Stabilization Approach for Deep-Space Optical Communications Terminals," *Proceedings of the IEEE*, vol. 95, no. 10, pp. 2070–2081, October 2007.

[13] A. Yariv, *Quantum Electronics*, New York: John Wiley and Sons, Inc., 3rd edition, 1989.

[14] B. E. A. Saleh and M. C. Teich, *Fundamentals of Photonics*, New York: John Wiley and Sons, Inc., 1991.